

Universal Robotic Gripper based on the Jamming of Granular Material: Supplementary material

Eric Brown¹ Nicholas Rodenberg¹, John Amend², Annan Mozeika³
Erik Steltz³, Mitchell R. Zakin⁴, Hod Lipson², Heinrich M. Jaeger¹

¹ James Franck Institute, The University of Chicago, Chicago, IL 60637

² School of Mechanical and Aerospace Engineering, Cornell University, Ithaca, NY 14853

³ iRobot G&I Research, 8 Crosby Drive, Bedford, MA 01730,

⁴ Defense Advanced Research Projects Agency, 3701 North Fairfax Drive, Arlington, VA 22203

In the main text we focused on vertical forces that pull along the central axis of the gripped object, i.e., along $\theta = 0$ in the sketch shown in Fig. 2a of the main text. However, the object may also experience torques or off-axis forces, which might arise in situations when the object's center of mass lies off the central axis, when the gripper holding the object is rotated, or when the gripped object collides with an obstacle. In this section we discuss the ability of the gripper to resist such off-axis forces and torques.

To measure the holding force of the gripper against off-axis forces we applied a force at $\theta = \pi/2$ in the radial direction toward the sphere center. To perform these tests, we embedded a solid test sphere of radius $R = 19$ mm as usual by first pushing it into the gripper to a pre-determined depth as shown in Fig. 2a in the main text. Next, the evacuated gripper holding the sphere was rotated by $\pi/2$ so the axis of cylindrical symmetry was horizontal (see inset to Fig. 2). In this configuration, force-displacement curves were taken with the Instron

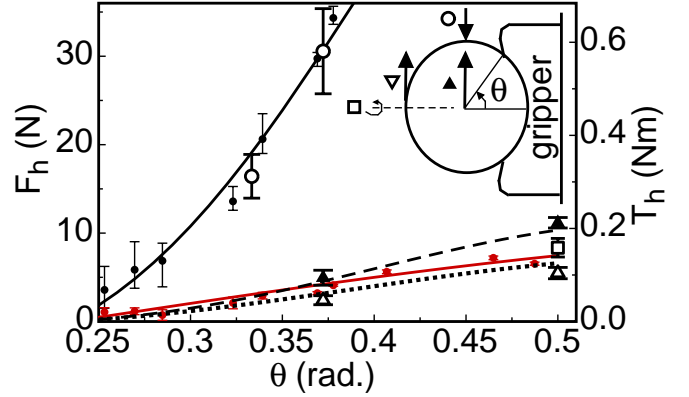


FIG. 2: Maximum holding forces F_h and torques T_h on different axes as a function of contact angle θ between $\pi/4$ and $\pi/2$. On-axis ($\theta = 0$) forces on the center of mass are reproduced from Fig. 3 of the main text for a porous sphere (red solid circles) and for a solid sphere (black solid circles), both at $P_{jam} = 80$ kPa. Solid lines give predictions as discussed in the main text. Off-axis forces applied to a solid sphere radially at $\theta = \pi/2$ are shown as open black circles. Torques are tested by pulling tangent to the edge of the sphere at radius R . Solid triangles: on-axis torques, with force applied tangent to the surface at $\theta = \pi/2$ and $P_{jam} = 80$ kPa. Open triangles: off-axis torques, with force applied tangent to the surface at $\theta = \pi$ and $P_{jam} = 80$ kPa. Open square: on-axis torque, measured by a rotating a key inserted into the sphere at $\theta = \pi$. Dashed and dotted lines: model for on-axis and off-axis torques at $P_{jam} = 80$ kPa, respectively, as discussed in the text. Inset: Diagram of the experimental setup, with arrows indicating the location and direction of applied forces for each measurement. The torque scale on the right is the force scale multiplied by R .

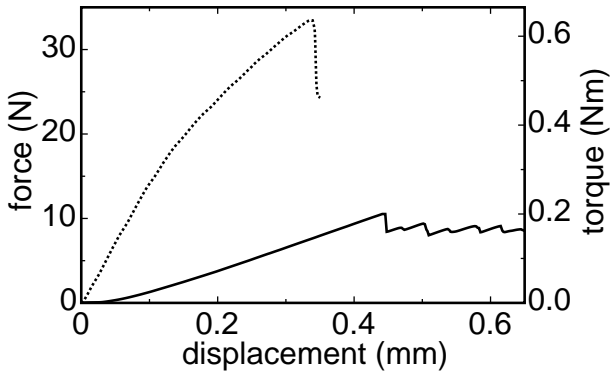


FIG. 1: Force-displacement curves for off-axis forces and torques. Dotted line: Off-axis force applied to a solid sphere radially at $\theta = \pi/2$ with a gripper contact angle $\theta = 0.37\pi$ and $P_{jam} = 80$ kPa. Solid line: On-axis torque applied by rotating a key inserted into the sphere at $\theta = \pi$, a contact angle of $\theta = \pi/2$, and $P_{jam} = 54$ kPa. The angular deflection has been converted to a displacement along the perimeter of the sphere by multiplying it by the sphere radius $R = 19$ mm. The torque scale on the right is the force scale multiplied by R , which corresponds to the maximum torque arm length of the friction applied by the gripper.

material tester by pushing a rod down onto the center of the sphere so it contacted at $\theta = \pi/2$. An example force-displacement curve is shown in Fig. 1. The maximum force before failure was designated, as before, as the holding force, F_h . Results for two contact angles are shown in Fig. 2. It is seen that the holding force against these off-axis forces is just as strong as in the case as on-axis forces discussed in the main text.

To test the holding force of the gripper against torques, we used the same sideways configuration for the gripper, and pulled on a string tied to the surface of the solid sphere, so the lever arm had the same length as the

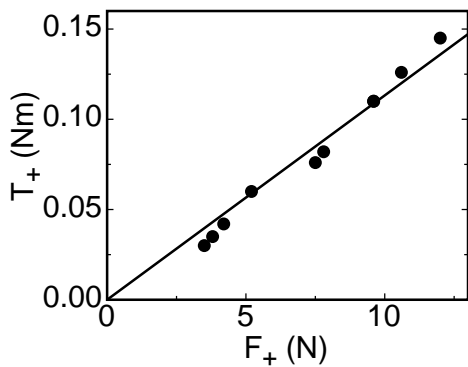


FIG. 3: Contribution T_+ to the holding torque due to normal forces F_+ between the gripper and sphere of radius $R = 19$ mm in addition to the holding torque provided by jamming. Solid line: a linear fit.

sphere radius. Data for the maximum holding torque, T_h , are shown in Fig. 2 for on-axis torques applied at an angle $\pi/2$ relative to the central gripper axis, and off-axis torques applied at an angle π . While this method of applying torques also introduced some net force, that force is significantly weaker than the off- and on-axis holding forces. Therefore, it is safe to conclude that failure was due to the torque and not the net force.

The forces for each torque measurement are in the range of the vertical holding force for frictional contact. Analytically, the torque applied by the gripper to hold the target in place cannot come from suction since that only provides forces normal to the surface of the sphere. Instead, the full effect of friction can be applied perpendicular to the torque arm. For on-axis torques, the torque arm around the center of the sphere is everywhere $R \sin \theta$, so the holding torque provided by friction is $T_h = F_f R \sin \theta$. For off-axis torques, the torque arm varies along the O-ring as $R |\cos \phi|$ where ϕ is the azimuthal angle around the gripper axis. The holding torque for off-axis torques is then $T_h = F_f R \int_0^{2\pi} |(\cos \phi)| d\phi / (2\pi) = 2F_f R / \pi$. For torques applied to the sphere at a radius of R , this predicts the same scale for the holding force F_f as found for forces on the center of mass. These models for the on- and off-axis torques are simultaneously fit to the data in Fig. 2, using the scale factor F_f as the only adjustable parameter (the resulting value of F_f is about 50% larger than the value found for the on-axis forces discussed in the main text; however, the values of F_f need not be the same because they are dependent on the contact area and this can vary as the gripper is deformed under different types of applied strain). Generally, this model implies that the center of mass of the load can be located off the central axis ($\theta = 0$) by as much as the mean radius of contact without a negative effect on the holding force.

In addition, we performed one more series of tests in which the sphere was twisted around the central axis while an external normal force was applied. Knowledge

about such on-axis torque is relevant in cases where the gripper is pushed onto an object and then rotated, for example in order to open a door by twisting a round knob. In these situations, the normal force can provide additional friction and thus enhance the maximum sustainable torque. For this measurement we used an Anton-Paar MCR 301 rheometer to measure both torque and angular deflection of a rotating tool while it applied a fixed normal force. The measuring geometry was similar to Fig. 2a in the main text, except in this case the vertical rod was replaced with the rheometer tool which was rotated around its axis rather than pulled. The rheometer tool was a cross-shaped key and was inserted into a matching slot on the top of a solid sphere with $R = 19$ mm.

To obtain a reference measurement with zero initial applied force in the normal direction, after pressing the sphere into the gripper and setting P_{jam} , we then back the key off slightly until the normal force reaches zero. An example torque-deflection curve in this setup with zero normal force is shown in Fig. 1 for a contact angle of $\theta = \pi/2$ and $P_{jam} = 54$ kPa. The maximum resulting holding torque, T_h , is shown in Fig. 2 (open square), where it is seen to be in good agreement with the other on-axis torque measurement when scaled by P_{jam} . Several stick-slip events are apparent in the torque-deflection curve. Note that, when the object is not also pulled out of the gripper, there is no permanent loss of grip after an initial slip. In fact, the stress recovers with a slope similar to the initial stress buildup.

To obtain results for different applied normal force values, we measured torque-deflection curves with the sphere pushed partially into the gripper by the rheometer. Many of these tests correspond to contact angles below $\pi/4$. Note that significant holding torques are found for small contact angles and even when $P_{jam} = 0$. We summarize these results by defining an extra holding torque, T_+ , which is the excess over the torque obtained in an equivalent experiment with zero applied normal force. This extra holding torque T_+ is plotted vs. the normal force at failure, F_+ , in Fig. 3. We note that F_+ can differ from the applied normal force at the beginning of the measurement by a few Newtons due to deformations in the gripper – it is specifically the normal force at failure that we find to be directly related to the holding torque. This additional contribution to the torque from the normal force is roughly proportional to F_+ , a relationship which holds for different values of contact angle and P_{jam} . T_+ can be attributed to friction and expressed as $T_+ = F_+ R \sin \theta_+$. Here θ_+ is a characteristic contact angle for the compression which is likely distributed over a wide area around the bottom of the sphere. The proportionality between T_+ and F_+ indicated by the solid line in Fig. 3 corresponds to $\theta_+ = 0.4\pi$. These results show that, given enough normal force, the gripper can achieve holding torques well above those produced by jamming alone.

Because we argued that the frictional force is more

than enough to lift any object on the scale of a few cm or less, our holding torque model suggests that the grip will not fail when the lifted object is rotated or picked up off-center. Furthermore, the displacement of the target in the gripper under off-axis forces shown in Fig. 1 was only $7\ \mu\text{m}$ at the point where the holding force equals the weight. Similarly, the stiffness to torque in the rheometer measurements was so large that even if the weight was distributed at the edge of the sphere, tilting would cause a deflection of only 0.001 radians or an edge displacement of $20\ \mu\text{m}$. These results show that the gripper is capable of precision holding during changes in orientation.

This discussion focusing on spheres can be extended to other shapes. The extreme case where there is a long lever arm on which torques can be most easily applied

is a horizontal rod longer than the gripper. The above analysis implies that the center of mass of the rod only needs to be somewhere within the space directly below the gripper for optimal gripping performance. If such a rod were gripped and then pushed along its axis, we would expect the gripper to respond with friction only since in this case suction would be entirely perpendicular to the applied force. However, suction could be operable in holding against torques in directions perpendicular to the rod axis, in which the lever arm is largest. For other shapes we would expect friction will provide a holding force against forces on any axis and some component of suction may be able to provide some holding force depending on target shape and force orientation.